Robust Dynamic Output Feedback Pitch Control for Flexible Wind Turbines

H. M. Hassan, W. A. Farag, M. S. Saad*, and Abdel Latif Elshafei

***Abstract*— This paper proposes a dynamic output feedback decentralized pitch controller for flexible wind turbines. Both collective and cyclic (individual) pitch controllers are considered. The collective pitch controller aims at improving the rotor speed regulation and maximizing the harvested electrical power, without violating the pitch actuator limits. On the other hand, the cyclic (individual) pitch controller targets mitigating the fatigue relevant loads caused by aerodynamic forces. Both controllers are designed based on a polytopic model. The design constraints include (H_∞ problem, H_2 problem and pole clustering). Initially an LMI-based feasible controller is designed, and then a final feasible controller is reached via local optimization iterative algorithm. The performance of the proposed controller is compared to a conventional PI-based controller. The results are validated by testing on a nonlinear flexible multi-MW wind turbine model against a realistic extreme turbulence wind profile.**

I. INTRODUCTION

The growing interest in wind energy makes it one of the most promising sources of renewable energy. With the worldwide desire of increasing the wind energy installed capacity, raising the turbines' size becomes an inevitable necessity. Nowadays, wind turbines reach magnificent sizes and become more flexible, and expected to get bigger. These giant turbines face a gigantic fatigue loads, especially, at above-rated wind speeds. These loads result from wind shear, turbulence, tower shadow, oblique inflow, and yaw misalignment. As a result, the pitch controller objective has been promoted from just harvesting the rated power to address the reduction of fatigue loads on the turbine structure. These objectives can be formulated in two control problems.

First problem is to design a collective pitch controller (CPC). A CPC regulates the generator speed to the rated value in order to harvest the rated electrical power without violating the pitch actuator limits. Moreover, the controller should perform satisfactorily in the presence of: nonlinearities in system dynamics; continuous change of the operating points during operation; and uncertainty due to unstructured dynamics. These difficulties motivate the need for designing a robust pitch controller that provides an accepted performance under such difficulties. Second problem is to design a cyclic (individual) pitch controller (IPC). An IPC main task is to alleviate the blades' flapwise moment. To address the two problems, a Combined CPC and IPC state feedback controller is recommended. Such controller is a well-known controller widely discussed in literature [1]-[5].

In [1], a PI-based CPC combined with a PI-based IPC is used for fatigue load reduction. In [2], a PI-based IPC is proposed combined with a gain scheduling feedback/feed-forward CPC. A different IPC design is proposed in [3], where an optimal LQG state feedback based design is used to minimization of the rotor tilt and yaw moments. In [4], an IPC is designed as H_∞ state feedback controller to enhance the damping of the tower displacement by reducing the blade flapwise bending moment. An H_∞ feedback/feed-forward CPC is discussed in [5] to get better disturbance rejection by minimizing the closed loop gain. The previous controllers are designed based on a single- operating model. In [6], a robust LMI-based state feedback CPC is presented; the controller takes parameters' uncertainty into consideration.

In this paper, a dynamic output-feedback-based CPC and IPC are proposed. The proposed controller addresses the following constraints; H_∞ criteria for better disturbance rejection, H_2 criteria for optimizing control action with performance, and Pole clustering for improving transient response. The controller is designed based on a polytopic model to account for model uncertainty at different operating points.

This paper is organized as follows; Section II discusses the turbine linearized models, and the decoupling between system states. Section III presents the proposed CPC and IPC design. In Section IV, simulation results to show the comparison between the proposed controller and a conventional PI-based controller are given. Finally, the conclusions are stated in Section V.

II. MODEL DESCRIPTION

In order to design a decentralized CPC and IPC, two decoupled designed models are needed. These models are derived in this section as follows; Part (a) presents the turbine's nonlinear model, and the corresponding linearized model. Part (b) presents the total design model by transferring the linearized model to a fixed frame, finally in part (c) we extract the desired decoupled models.

- All authors are with the department of Electrical Power and Machines, Cairo University, EGYPT.
* Corresponding author (email: mssaad@eng.cu.edu)

a. Linearized models

The wind turbine is modeled using a full non-linear time variant model provided by FAST (Fatigue, Aero-dynamics, Structures, and Turbulence). This software code is developed at the US National Renewable Energy Laboratory (NREL) [7]. FAST model has the following form;

$$M\,(q,u,t)\ddot{q} \;+\; f\,(\dot{q},q,u,u_d,t) = \;0, \quad y \;=\; h\,(\dot{q},q,t)\ (1)$$

where M is the turbine mass matrix, f is the nonlinear "forcing function" vector, q is the vector of degrees of freedoms (DOFs) displacements, u is the vector of control inputs, u_d is the vector of disturbances, and t is the time. The model used here is a 3-bladed, variable speed 5 MW wind turbine model with rated generator speed equals (1174 rpm). Important specifications are given in the appendix. Further specifications are mentioned in [8]. A pitch actuator model is also included in the design. It is represented as a second order model. The permissible pitch angle ranges from 0- 90° with a maximum rate of 8°/s.

FAST can provide a linearized model around a certain operating point λ. An operating point λ is identified through $(\Psi, \bar{\omega}_{gen}, \bar{\theta}, \bar{v}_w)$, where Ψ is the rotor's azimuth angle, $\bar{\omega}_{gen}$ is the generator speed, $\bar{\theta}$ is the pitch angle, and $\bar{v}_w$ is the hub height wind speed. The resulting azimuth-dependent linear model is as follows:

$$M(\psi)\Delta\ddot{q} + C(\psi)\Delta\dot{q} + K(\psi)\Delta q = F(\psi)\Delta u + \; F_d(\psi)\Delta u_d$$
$$y = c_v(\psi)\Delta\dot{q} + c_d(\psi)\Delta q \qquad (2)$$

where Δ denotes the deviation from the operating point and it will be omitted from now on for simplicity. C and K denote stiffness, and damping matrix, respectively. The control vector is $u = [\theta_1, \theta_2, \theta_3]^T$, where θ_i denotes the pitch angle of the i[th] blade. The output vector y is defined as $y = [\omega_{gen}, M_{Flp1}, M_{Flp2}, M_{Flp3}]^T$where M_{Flpi} denotes the flapwise moment measured at the tip of the i[th] blade. The state vector $q = [q_{Gen}, q_{DT}, q_{FLP1}, q_{FLP2}, q_{FLP3}]^T$, where q_{Gen} , q_{DT}, q_{FLB1}, q_{FLB2}, q_{FLB3} denote the displacements of the generator, the drivetrain rotational-flexibility, and the flapwise blade mode for each blade DOFs, respectively. The different DOFs in FAST are depicted in Fig.1

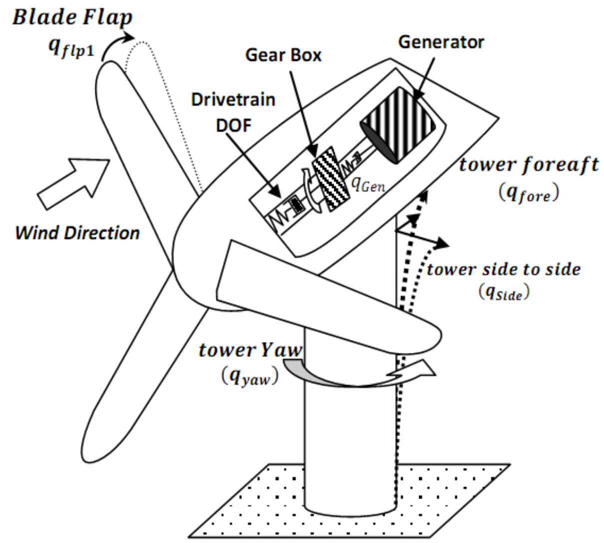

Fig. 1. Different DOFs in flexible wind turbine

Some DOFs belong to a fixed frame; (q_{Gen} , q_{DT}), others belong to a rotating frame (q_{FLB1}, q_{FLB2}, q_{FLB3}), which depend on Azimuth angle Ψ. In order to control all DOFs from the fixed frame, multi-blade coordinate transformation (MBC) must be performed to those DOFs belonging to the rotating frame [10].

b. Multi-blade Coordinate Transformation (MBC)

In order to transfer the states and the output vectors $y_{rt} = [M_{Flp1}, M_{Flp2}, M_{Flp3}]^T, \quad q_{rt} = [q_{flp1}, q_{flp2}, \; q_{flp3}]^t$ into a fixed frame, inverse Colman (d-q) transformation is used [10]. It transfers the rotating frame's vectors (q_{rt}, y_{rt}) into a fixed frame's vectors (q_{fx}, y_{fx}) depicted in Fig. 2.

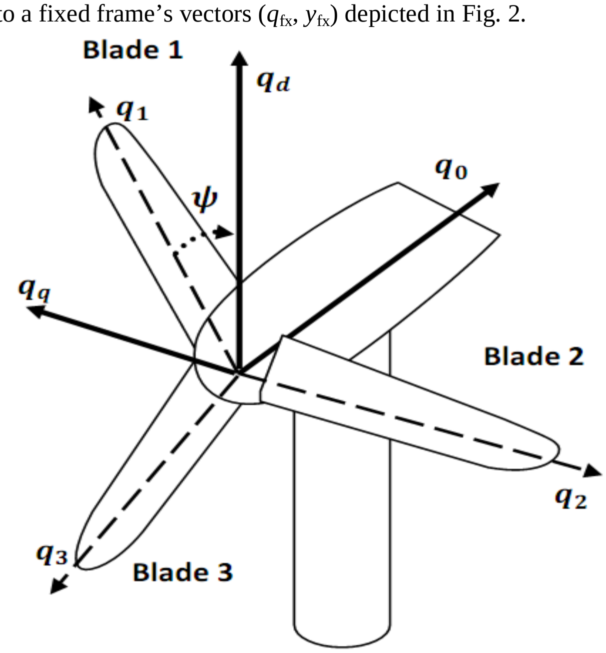

Fig. 2. Multi blade coordinate transformation

The fixed frame is defined by three components; synchronous component denoted with *0*, sine (quadratic) and cosine (direct) which are indexed by q and d respectively. The fixed frame is given as;

$$y_{fx} = [M_0, M_d, M_q]^T \quad q_{fx} = [q_{flp0}, q_{flpd},\ q_{flpq}]^t$$

The transformation matrix T^{-1} is defined as:

$$T^{-1} = \frac{2}{3} * \begin{pmatrix} 0.5 & 0.5 & 0.5 \\ cos(\psi) & \cos(\psi+\frac{2\pi}{3}) & \cos(\psi+\frac{4\pi}{3}) \\ \sin(\psi) & \sin(\psi+\frac{2\pi}{3}) & \sin(\psi+\frac{4\pi}{3}) \end{pmatrix} \quad (3)$$

$$q_{fx} = T^{-1} \times q_{rt} \quad y_{fx} = T^{-1} \times y_{rt}$$

Model (2) linearized around certain operating point λ, $\lambda = (\bar{\omega}_{gen}, \bar{\theta}, \bar{v}_w)$ referred to the fixed frame can be rewritten as;

$$M_{0dq}\ddot{q}_{0dq} + C_{0dq}\dot{q}_{0dq} + K_{0dq}q_{0dq} = F_{0dq}u_{0dq} + F_{d\,0dq}u_{d\,0dq} \quad (4)$$
$$y_{odq} = C_{v\,0dq}\dot{q}_{0dq} + C_{d\,0dq}q_{0dq}$$

where $q_{0dq} = [q_{Gen}, q_{DT}, q_{fx}]^T$, $y_{odq} = [\omega_{gen}, y_{fx}]^T$. The derivation of the fixed frame's matrices is given in [10]. To transfer the control output $u_{0dq} = [\theta_0, \theta_d, \theta_q]^T$ from the fixed frame to $u_{rt} = [\theta_1, \theta_2, \theta_3]^T$ in the rotating frame, inverse D-q transformation can be used as follows;

$$u_{rt} = T \times u_{odq} \quad (5)$$
$$T = \begin{bmatrix} 1 & cos(\psi) & \sin(\psi) \\ 1 & \cos(\psi+\frac{2\pi}{3}) & \sin(\psi+\frac{2\pi}{3}) \\ 1 & \sin(\psi+\frac{2\pi}{3}) & \sin(\psi+\frac{2\pi}{3}) \end{bmatrix}$$

c. The decoupled fixed frame model

As proposed in [11], the following decoupling is possible;

$$\begin{bmatrix} M_0 & 0 \\ 0 & M_{dq} \end{bmatrix}\ddot{q}_{0dq} + \begin{bmatrix} C_0 & 0 \\ 0 & C_{dq} \end{bmatrix}\dot{q}_{0dq} + \begin{bmatrix} K_0 & 0 \\ 0 & K_{dq} \end{bmatrix}q_{0dq} = \begin{bmatrix} F_0 & 0 \\ 0 & F_{dq} \end{bmatrix}u_{0dq} + \begin{bmatrix} F_{d\,0} & 0 \\ 0 & F_{d\,dq} \end{bmatrix}u_{d\ 0dq}$$
$$y_{odq} = \begin{bmatrix} c_{v\,0} & 0 \\ 0 & c_{v\,dq} \end{bmatrix}\dot{q}_{0dq} + \begin{bmatrix} c_{d\,0} & 0 \\ 0 & c_{d\,dq} \end{bmatrix}q_{0dq} \quad (6)$$

By this decoupling, it is possible to simplify the fixed frame model in (4) to get two design models at a given operating point λ ; $p_0(\lambda)$, and $p_{dq}(\lambda)$. $p_0(\lambda)$ represents the synchronous component (azimuth-independent states), $p_0(\lambda)$ takes the form;

$$p_0(\lambda): \begin{cases} \dot{x} = Ax + Bu + B_d u_d \\ y = Cx + Du + D_d u_d \end{cases} \quad (7)$$

where $x = [x_{DT}, x_{Gen}, \dot{x}_{DT}]^T$
x_{DT}: Perturbation in Drivetrain torsional displacement (which reflects the drivetrain rotational-flexibility); (m)
x_{Gen} : Perturbation in rotor speed; (rad/s)
$\dot{x}_{DT}$: Perturbation in Drivetrain torsional velocity; (m/s)
$u = [\theta_0]$ is the perturbation in the collective pitch (control action), $u_d = [v_w]$ is the perturbation in the wind speed, $y = [\omega_{gen}]$ is the perturbation in generator speed. $p_0(\lambda)$ is a continuous model with minimum phase behavior. It is completely observable and controllable. The synchronous component model $p_0(\lambda)$ will be used in designing the CPC.

The decoupled model $p_{dq}(\lambda)$ represents the (d-q) components. $p_{dq}(\lambda)$ takes the following form;

$$p_{dq}(\lambda): \begin{cases} \dot{x} = Ax + Bu + B_d u_d \\ y = Cx + Du + D_d u_d \end{cases} \quad (8)$$

Where $x = [x_d, x_q, \dot{x}_d, \dot{x}_q]^T$
x_d: rotor tip-path-plane fore-aft tilt , perpendicular to the rotor shaft's axis; (m)
x_q : rotor tip-path-plane side-side tilt normal to the rotor shaft's axis; (m)
$\dot{x}_d$: rotor tip-path-plane fore-aft velocity, perpendicular to the rotor shaft's axis; (m/s)
$\dot{x}_q$: rotor tip-path-plane side-side velocity normal to the rotor shaft's axis; (m/s)
u = $[\theta_d \quad \theta_q]$, $y = [M_d, M_q]$ where M_d, M_q, are the direct, quadratic moments, respectively. $p_{dq}(\lambda)$ is a continuous model. It is completely observable and controllable. The (d-q) model $p_{dq}(\lambda)$ will be used in designing the IPC.

III. CONTROLLER DESIGN

The proposed control synthesis is depicted in Fig. 3.

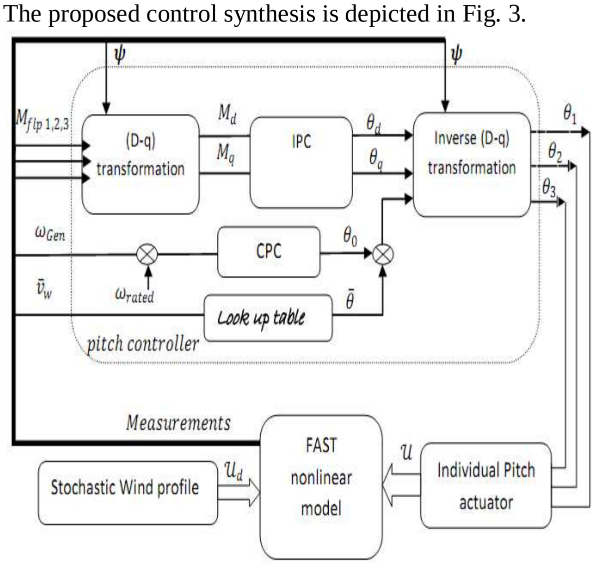

Fig. 3. Controller synthesis

The proposed Control strategy is to design decentralized CPC and IPC. Both controllers are robust, Dynamic-output-feedback-based. The total control action u is calculated as follows:

$$u = \bar{\theta} + u_{rt} = T \times \left[\bar{\theta} + \theta_0 \quad , \theta_d \quad \theta_q\right]^T \tag{9}$$

where $\bar{\theta}$ is the pitch angle operating point. It changes with the wind speed $\bar{v}_w$, and is calculated using a lookup table

1. Designing the CPC

The main controller's objective is the robustness of the system given in (7), at different operating points $\lambda_i: \lambda_i = (\bar{\omega}_{gen}, \bar{\theta}_i, \bar{v}_{w_i})$. Thus, six different models are derived at different wind speeds along the operating range (which ranges from 12 m/s to 25 m/s). The selected speeds are ($\bar{v}_w = 12\, m/s, 14\, m/s, 16\, m/s, 18\, m/s, 20\, m/s, 22\, m/s$). Each model represents a different operating point with a unique pitch angel $\bar{\theta}_i$. All the models are linearized at the rated generator speed ($\bar{\omega}_{gen}$). The polytopic model is defined by a convex envelope Ω_0 which is defined as;

$$\Omega_0 = Co\{p_0(\lambda_1), \dots, p_0(\lambda_6)\}$$
$$\Omega_0 = \left\{\sum_{i=1}^{6} \alpha_i p_0(\lambda_i): \alpha_i \geq 0, \sum_{i=1}^{6} \alpha_i = 1\right\}$$
$$, p_0(\lambda_i): \begin{cases} \dot{x} = A_i x + B_i u + B_{d_i} u_d \\ y = Cx + Du + D_d u_d \\ Z_\infty = C_\infty x + D_\infty u \\ Z_2 = C_2 x + D_2 u \end{cases} \tag{10}$$

Three constraints are addressed to achieve the required CPC objectives:

1- Efficient disturbance rejection for better speed regulation addressed by H_∞ problem [12]. This constraint aims at keeping the RMS gain of $T(s)_\infty$ (H_∞ norm) below a predefined value γ, ($\gamma > 0$), where $T(s)_\infty$ is the closed loop transfer function from u_d to Z_∞, where $Z_\infty = x_{Gen}$, represents the regulation error due to disturbance u_d.

2- The trade-off between the control effort and the performance is addressed by H_2 problem [12]. This constraint minimizes a cost function (J) that reflects a weighted sum of the control effort and states' perturbations,

$$J = \int_0^\infty {c_2}^2 x^2 + {D_2}^2 u^2 dt \tag{11}$$

The minimization is carried out by keeping the H_2 norm (LQG Cost) of $T(s)_2$ below a predefined value β,($\beta > 0$), where $T(s)_2$ is the closed loop transfer function from u_d to Z_2.

3-Achieving a desired transient response is fulfilled by maintaining the closed loop poles of (13) inside a particular region D. This constraint is addressed as a pole clustering problem [13]. Region D is defined as $D = \{z \in c: \pi + \Gamma z + \Gamma^T \bar{z} < 0\}$, where ($\Gamma$, π) are the region matrices, depending on the region shape, and c is the complex plane.

In this paper, D is proposed to be the intersection between three regions (R_1, R_2, and R_3). The first region R_1 guarantees an upper limit on settling time. The second region R_2 guarantees a lower limit on settling time (which prevents excessive control action). $R_1$and R_2 regions are defined in s-plane by a vertical strip bounded by (h_1, h_2), and defined by the region matrices (π_1, Γ_1). Region R_3 is chosen as an upper bound on damping. R_3 is a conic sector centered at the origin with inner angle (2φ) and defined by the region matrices (π_2, Γ_2). The region's characteristic function is given in [14]. The form of a full order robust Output feedback controller is;

$$CPC \begin{cases} \dot{\xi} = A_k \xi + B_k y \\ u = C_k \xi \end{cases} \tag{12}$$

The resulting augmented model is:

$$p_{0cl}(\lambda_i): \begin{cases} \dot{x}_{cl} = A_{icl} x_{cl} + B_{icl} u_d \\ Z_\infty = C_{cl\infty} x_{cl} \\ Z_2 = C_{cl2} x_{cl} \end{cases} \tag{13}$$
$$where\ , A_{icl} = \begin{bmatrix} A_i & B_i C_k \\ B_k C & A_k \end{bmatrix} \quad x_{cl} = [x^T \quad \xi^T] \quad B_{icl} = [B_d^T \quad 0]^T$$
$$C_{cl2} = [C_2 \quad D_2 C_k] \quad C_{cl\infty} = [C_\infty \quad D_\infty C_k]$$

By making the nonlinear transformation proposed in [15] for the augmented model, we convert the constraints inequalities into affine ones in the controller parameters. Define a Lyapunov matrix P that should fulfill all the design constraints;

$$P = \begin{bmatrix} Y & N \\ N^T & Z \end{bmatrix} \quad P^{-1} = \begin{bmatrix} X & M \\ M^T & V \end{bmatrix} \tag{14}$$

The transferred variables are indexed with (v) as follows;

$$A_i(v) = \begin{bmatrix} A_i X + B_i \hat{C} & A_i \\ Y A_i X + Y B_i \hat{C} + \hat{A} & Y A_i + \hat{B} C \end{bmatrix} \quad P(v) = \begin{bmatrix} X & I \\ I & Y \end{bmatrix}$$
$$B(v) = \begin{bmatrix} B_{di} \\ Y B_{di} \end{bmatrix} \quad \begin{matrix} c_2(v) = [c_2 X + D_2 \hat{C} \quad C_2] \\ c_\infty(v) = [c_\infty X + D_\infty \hat{C} \quad C_\infty] \end{matrix} \tag{15}$$

Where: $\hat{A} = N A_k M^T + N B_K C X$, $\hat{B} = N B_K \quad \hat{C} = C_k M^T$

CPC is constructed to solve the following problem [15];

$$\min_{(X, Y, Q, \hat{A}, \hat{B}, \hat{C})}(\gamma) \quad subject\ to:$$
$$H_2 \text{ problem} \begin{cases} \begin{bmatrix} A_i(v) + A_i(v)^T & B(v) \\ * & -I \end{bmatrix} < 0 \\ \begin{bmatrix} Q & c_2(v) \\ * & P(v) \end{bmatrix} > 0 \\ Trace(Q) < \beta^2 \end{cases} \tag{16}$$

$$H_\infty \text{ problem}\left\{\begin{bmatrix} A_i(v)+A_i(v)^T & B(v) & c_\infty(v)^T \\ * & -\gamma I & 0 \\ * & * & -\gamma I \end{bmatrix}\right. \quad (17)$$

$$pole\ clust.\begin{cases}\pi_1 \circledast P(v)+\Gamma_1 \circledast A_i(v)+\Gamma_1{}^T \circledast A_i(v)^T<0 \\ \pi_2 \circledast P(v)+\Gamma_2 \circledast A_i(v)+\Gamma_2{}^T \circledast A_i(v)^T<0\end{cases} \quad (18)$$

Such that $XY+MN^T=I$, where (*) denotes a symmetrical element, ($\circledast$) denotes the kroneker product. The resulting controller is:

$$C_k=\hat{C}M^{-T} \quad B_k=N^{-1}\hat{B}$$
$$A_k=N^{-1}(\hat{A}-NB_kCX)M^{-T} \quad (19)$$

The above problem's constraints contain bi-linear terms. Different approaches exist for solving this problem. These approaches are classified as global [16], and local [17]. The global approach is known to be a non-convex NP-hard optimization problem. It is normally done by variations of the branch and bound [16]. Although the local approaches may not converge to the global optimum, it is faster than the global approach. In this paper the local optimization approach will be adopted. The optimization approach is carried out in two steps. Step (A), where an initial feasible controller is derived as proposed in [17]. Step (B), where the final controller is reached via a local optimization iterative algorithm. The algorithm depends on fixing some variables in order to get convex constraints.

Step A. Finding an initial feasible controller

To find an initial feasible controller; first, a state feedback controller *u: u*=*k x* is designed. This controller addresses all the desired constraints for the polytopic model. This problem is defined by LMI-constraints given in [13]. Second, solve the following problem:

given $C_K=k$; $\min_{(X,Y,Q,G,Z)}(\gamma)$ $subject\ to$:

$$H_\infty \text{ problem}\left\{\begin{bmatrix} M_i+M_i{}^T & PB_{cl} & c_{cl\infty}{}^T \\ * & -\gamma I & 0 \\ * & * & -\gamma I \end{bmatrix}\right. \quad (20)$$

$$H_2 \text{ problem}\begin{cases}\begin{bmatrix} M_i+M_i{}^T & PB_{cl} \\ * & -I\end{bmatrix}<0 \\ \begin{bmatrix} Q & c_{cl2} \\ * & P(v)\end{bmatrix}>0 \\ Trace(Q)<\beta^2\end{cases} \quad (21)$$

$$pole\ clust.\begin{cases}\pi_1 \circledast P(v)+\Gamma_1 \circledast M_i+\Gamma_1{}^T \circledast M_i{}^T<0 \\ \pi_2 \circledast P(v)+\Gamma_2 \circledast M_i+\Gamma_2{}^T \circledast M_i{}^T<0\end{cases} \quad (22)$$

Such that $XY+MN^T=I$, where

$$M_i=\begin{bmatrix} X(A_i+B_iC_K) & -XB_iC_K \\ Y(A_i+B_iC_K)-Z-GC & Z-YB_iC_K\end{bmatrix} \quad PB_{cl}=\begin{bmatrix} XB_{di} \\ YB_{di}\end{bmatrix}$$
$$c_{cl2}=[c_2+D_2C_K \quad -D_kC_2] \quad c_{cl\infty}=[c_\infty+D_\infty C_K \quad -D_kC_\infty]$$

The resulting controller is:

$$B_k=Y^{-1}G \quad A_k=Y^{-1}G \quad (23)$$

Step B. Concluding the final controller

The final controller is reached by the following algorithm;
Step (1); Find initial feasible controller as in step A, then define; $X_0=X_k \quad Y_0=Y_k \quad \hat{C}_0=\hat{C}$
Step (2); set *j*=1.
Step (3); by setting ($X=X_{j-1} \quad \hat{C}=\hat{C}_{j-1}$) in (14), we get the following convex LMI problem;

$$\left(Y_j,\gamma^x{}_j\right)=\arg\min\{(\gamma)\ subject\ to:(16,17,18)\} \quad (24)$$

Step (4); by setting ($Y=Y_{j-1}$) in (14), we get the following convex LMI problem;

$$\left(X_j,\hat{c}_j,\gamma^y{}_j\right)=\arg\min\{(\gamma)\ subject\ to:(16,17,18)\} \quad (25)$$

Step (5); If ($\gamma^y{}_j-\gamma^x{}_j>\varepsilon$) then set $j=j+1$, go back to step (3), where ε is a prescribed tolerance for the cost (γ) . Else, we conclude the final controller from (19).

2. Designing IPC

The main controller's objective is the robustness of the system $p_{dq}(\lambda)$ at different operating points $\lambda_i=(\bar{\omega}_{gen},\bar{\theta}_i,\bar{v}_{w_i})$. Thus, six different models are derived at the aforementioned wind speeds. All the models are linearized at the rated generator speed. The polytopic model is defined by the convex envelope Ω_{dq}.

$$\Omega_{dq}=Co\{p_{dq}(\lambda_1),\ldots,p_{dq}(\lambda_6)\}$$
$$\Omega_{dq}=\left\{\sum_{i=1}^{6}\alpha_i p_{dq}(\lambda_i):\alpha_i\geq 0,\sum_{i=1}^{6}\alpha_i=1\right\}$$
$$p_{dq}(\lambda_i):\begin{cases}\dot{x}=A_ix+B_iu+B_{d_i}u_d \\ y=Cx+Du+D_du_d \\ Z_\infty=C_\infty x+D_\infty u\end{cases} \quad (26)$$

The spectrum of the blade root bending moment has a dominant component at frequency 1p (once per revolution), with higher harmonics are of insignificant values as stated in [3]. Two constraints are addressed to achieve the required IPC objectives;

1-H_∞ problem; ($\|T(s)_\infty\|_\infty<\gamma$). This is accomplished by minimizing the H_∞ gain from external disturbance signals $u_d$to the desired performance output Z_∞: $Z_\infty=[M_d,M_q]$

2- Pole clustering problem; improving the transient response by maintaining the closed loop poles inside a particular region *D.* As stated in the CPC design section, the resulting region *D* is the intersection between a conic sector used to define the desired damping, and a vertical strip used to define the desired upper, and lower limit of the settling time.

Unlike the CPC design, IPC's control action does not exert high stress on the Pitch actuator. Thus, H_2 problem is not addressed in the design constraints. Designing procedures are the same as CPC. This is possible by following steps from (12) to (25) and omitting the H_2 problem constraints steps.

IV. SIMULATION RESULTS

The proposed controller is tested on a flexible wind turbine simulator using FAST. The testing is carried out on two wind profiles. The first is step change wind profile and shown in Fig. 4. The second is a fifty year Extreme turbulence wind profile and shown in Fig. 5. It is an IEC standard full field wind profile developed by TurbSim wind simulator [18] to reflect the toughest wind profile ever .turbine flexibility is simulated by enabling eight DOFs during simulation on FAST model. These DOFs are depicted in Fig. 1. They include the Drivetrain rotational-flexibility, the generator, the first flapwise bending of each blade, the yaw, the First fore-aft tower bending, and First side-to-side tower bending DOFs. The controller's performance is compared with a fine tuned PI-based CPC. The resulting gains of PI are (K_P=0.0018, K_I = 0.001779). The PI-based controller represents the most common controller used in commercial turbines. In our comparison, PI controller is derived using MATLAB Control system toolbox [19]. It is based on single model derived at $\overline{v}_w = 18\,m/s$. Fig. (4) depicts this comparison.

The first controller's comparison is for flexible turbine with step change wind profile (starting form 12 m/s and increasing by 2m/s each 20 second). Fig. 4 shows the results.

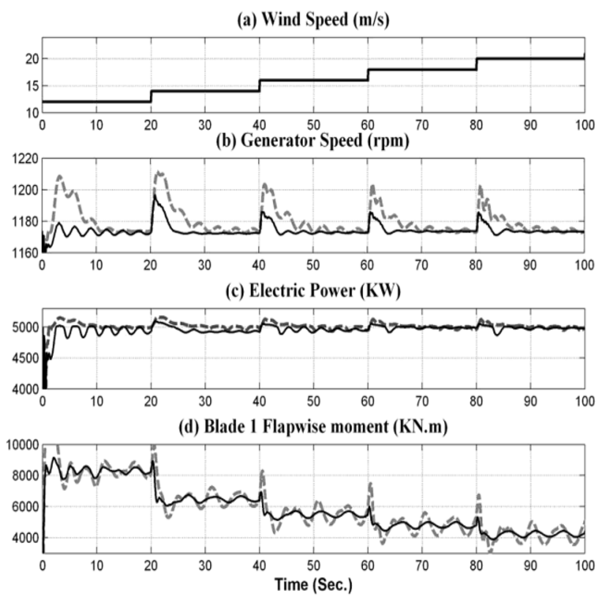

Fig. 4 Comparison results between; PI controller (gray dotted line), and the proposed controller (black solid line)

Fig. 4 shows the privilege for the proposed controller (solid black) over the PI controller (gray dotted). The proposed controller has higher damping and better transient response at different operating points (wind speeds). To get creditability in the comparison, a realistic wind profile is used. In Fig. 5, both controllers are tested on flexible wind turbine under extreme turbulence wind profile.

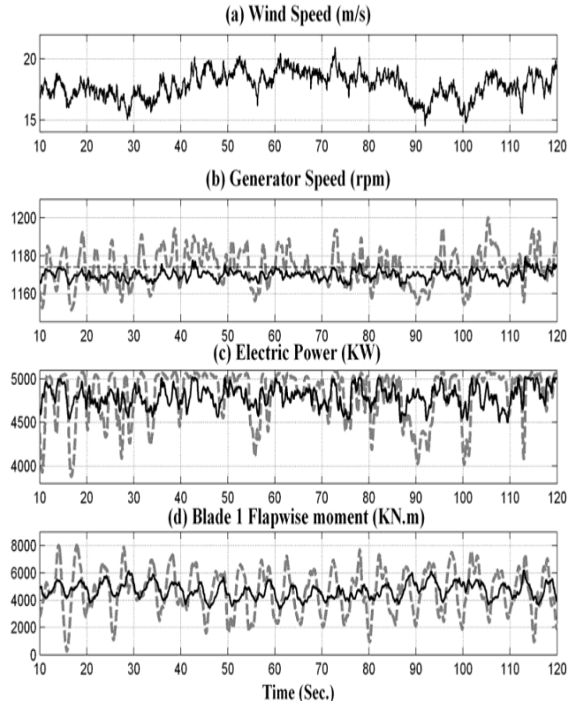

Fig. 5. Comparison results between; PI controller (gray dotted line), and the proposed controller (black solid line)

For Fig. 5 results, table 1 shows a Comparison between both controllers in terms of Speed and power regulation.

Table 1. Speed and power comparison

		PI	LMI
Generator speed (% of the rated speed)	Max.	102%	100.4 %
	Mean	100.1%	99.9%
	Std. dev.	10 rpm	2 rpm
Electric power (% of the rated power)	Max.	103 %	100.5%
	Mean	96%	96.3%
	Std. dev.	300 KW	100 KW

Table 1 shows that the proposed controller has improved the speed regulation significantly. This comes out in the massive reduction of the speed's standard deviation (five folds reduction). Moreover, the generator's maximum speed is reduced. On the other hand, the harvested power profile has improved significantly. The proposed controller has improved the power quality. The profile has become more flat and the power dips have been reduced significantly. The standard deviation of the power has been reduced by three times with such a severe wind profile. Although the mean harvested power has improved slightly, the maximum power has reduced significantly. This prevents generator overloading. As a result, the generator keeps working within permissible rated values. The flapwise moment is compared for both controllers in Table 2.

Table 2. Flapwise moment Comparison

	PI	IPC
Max	8020 KN.m	6190KN.m
Range (Peak to Peak)	7760 KN.m	2800 KN.m
Std. dev.	1600 KN.m	570 KN.m

The comparison shows the superiority of using the proposed controller over the PI controller. The conventional PI controller is a collective pitch controller. It can't reduce the cyclic mechanical fatigue loads. On the other hand, the proposed IPC has managed to reduce the cyclic loads significantly by alleviating the (1P) frequency loads, as shown in Fig. 6. The high standard deviation reduction ensures this (three folds reduction). More important, the proposed IPC has managed to reduce the maximum load significantly (25% reduction in maximum flapwise moment). Thus, the turbine keeps working in the safe-side range of operation according to the turbine dynamics constraints stated in [20]. This leads to minimization of maintenance cost, and an increase in the turbine's life time**.**

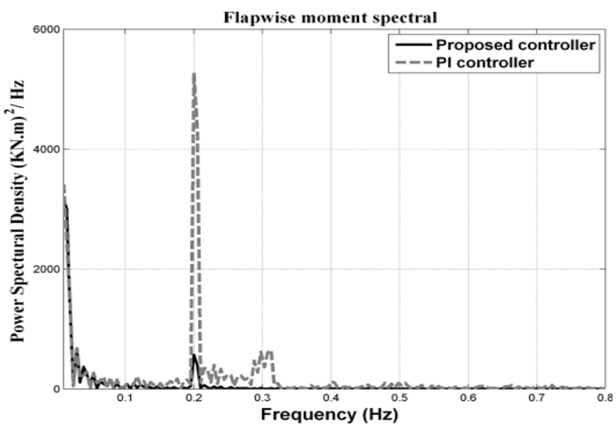

Fig. 6. Flap blade rotor bending moment power spectral; PI controller (gray dotted line), and the proposed controller (black solid line)

V. CONCLUSION

This paper proposes a decentralized robust pitch controller. It is a Multi-objective Dynamic Output feedback based on polytopic model. The design constraints have included H_∞ problem, H_2 problem, and pole clustering .A comparison with PI controller shows that the proposed controller has accomplished significant results in terms of improving speed regulation (five folds reduction in speed regulation error), increasing power quality (three folds reduction in the power regulation error), and mitigating fatigue loads; (25% reduction in the maximum flapwise moment).

APPENDIX

The Turbine's specifications are given in Table 3.

Table 3. Turbine's specifications

Hub height, Blade's diameter	90 meter, 126 meter
Cut in, Rated, cut out wind speed	3 m/s , 11.4 m/s, 25 m/s
Cut in, Rated generator speed	669 rpm, 1173.7rpm
Rotor, Tower, nacelle mass	110 ton, 347.4 ton, 240ton

REFERENCES

[1] David G. Wilson, Dale E. Berg,Brian R. Resor, Matthew F. Barone, Jonathan C. Berg, " Combined Individual Pitch Control and Active Aerodynamic Load Controller Investigation for the 5MW UpWind Turbine". *AWEA WINDPOWER 2009 Conference & Exhibition, Chicago, Illinois*, May 4-7, 2009.

[2] Fiona Dunney, Lucy Y. Paoz, Alan D. Wrightx, Bonnie Jonkman, Neil Kelle, "Combining Standard Feedback Controllers With Feed forward Blade Pitch Control for Load Mitigation in Wind Turbines," *in Proc. 48th AIAA Aerospace Sciences Meeting, Orlando, FL,AIAA-2010-250, Jan. 2010*

[3] K. Selvam, S. Kanev, J. W. vanWingerden, T. van Engelen, and M. Verhaegen, "Feedback feed forward individual pitch control for wind turbine load reduction," *Int. J. Robust Nonlinear Control*, 2008.

[4] M. Geyler,P. Caselitz, "individual blade pitch control for load reduction on large wind turbines", *Proceedings of the European Wind Energy Conference, Milan, Italy, 2007*.

[5] Jason Laks z, Lucy Paox, Alan Wright," Combined Feed-forward Feedback Control of Wind Turbines to Reduce Blade Flap Bending Moments", *AIAA Proceedings*, Jan 2009.

[6] Christoffer Sloth, Thomas Esbensen, Michael O.K. Niss, Jakob Stoustrup, and Peter F. Odgaard," Robust LMI-Based Control of Wind Turbines with Parametric Uncertainties", *18th IEEE Inter. Conf. on Control Applications, , Russia, July 8-10, 2009***.**

[7] Jonkman, J., and Buhl, M. L., Jr., "FAST Users Guide" National Renewable Energy Laboratory, NREL/EL-500-38230, Golden, CO, August 2005.

[8] Jonkman, J., Buttereld, S., Musial, W., and Scott, G., "Definition of a 5-MW Reference Wind Turbine for Offshore System Development" National Renewable Energy Laboratory, NREL/TP-500-38060, *Golden, CO*, February 2009.

[9] Gunjit S. Bir," Multi-blade Coordinate Transformation Utility for 3-Bladed Wind Turbines", Technical report, NREL, October 2008.

[10] E.A. Bossanyi, "Individual blade pitch control for load reduction", *Wind Energy*, pp. 119–128, 2003.

[11] M. Geyler and P. Caselitz, "Robust multivariable pitch control design for load reduction on large wind turbines," *ASME Journal of Solar Energy Engineering, vol. 130*, 2008.

[12] Kemin zoo," Essentials of Robust Control". *Printice Hall, 1997*.

[13] M. Chilali and P. Gahinet." H_∞ design with pole placement constrains: an LMI approach." *IEEE Trans. Automatic Control*, pp. 358-367, 1996**.**

[14] J Chilali, M., Ghainet. "Robust pole placement in LMI regions." *IEEE Trans. Automatic Control*, pp. 2257-2269, Dec. 1999.

[15] Carsten Scherer, Pascal Gahinet, and Mahmoud Chilali, "Multi-objective Output-Feedback Control via LMI Optimization", *IEEE Trans. on Automatic Control*, VOL. 42, NO. 7, JULY 1997.

[16] Fukuda, M., & Kojima, M.,"Branch-and-cut algorithms for the bilinear matrix inequality Eigen value problem". *Computational Optimization and Applications*, vol. 19, pp. 79-105, 2001.

[17] S. Kanev, C. Scherer, M. Verhaegen , B. De Schutter. "Robust output-feedback controller design via local BMI optimization". *Automatica*, Vol. 40, pp. 1115 – 1127, 2004.

[18] Kelley, N. D., and Jonkman, B. J.," Overview of the TurbSim Stochastic In flow Turbulence Simulator." *NREL*, April 2007.

[19] "Control System Toolbox User's Guide", Math works Inc., 1999.

[20] J.M. Jonkman, "Dynamics Modeling and Loads Analysis of an Offshore Floating Wind Turbine", *technical Report*, NREL/TP-500-41958, November 2007.